

## Measurement of Excited States in $^{40}\text{Si}$ and Evidence for Weakening of the $N = 28$ Shell Gap

C. M. Campbell,<sup>1,2</sup> N. Aoi,<sup>3</sup> D. Bazin,<sup>1</sup> M. D. Bowen,<sup>1,2</sup> B. A. Brown,<sup>1,2</sup> J. M. Cook,<sup>1,2</sup> D.-C. Dinca,<sup>1,2</sup> A. Gade,<sup>1,2</sup> T. Glasmacher,<sup>1,2</sup> M. Horoi,<sup>4</sup> S. Kanno,<sup>5</sup> T. Motobayashi,<sup>3</sup> W. F. Mueller,<sup>1</sup> H. Sakurai,<sup>3</sup> K. Starosta,<sup>1,2</sup> H. Suzuki,<sup>6</sup> S. Takeuchi,<sup>3</sup> J. R. Terry,<sup>1,2</sup> K. Yoneda,<sup>3</sup> and H. Zwahlen<sup>1,2</sup>

<sup>1</sup>National Superconducting Cyclotron Laboratory, Michigan State University, East Lansing, Michigan 48824, USA

<sup>2</sup>Department of Physics and Astronomy, Michigan State University, East Lansing, Michigan 48824, USA

<sup>3</sup>The Institute of Physical and Chemical Research, 2-1 Hirosawa, Wako, Saitama 351-0198, Japan

<sup>4</sup>Physics Department, Central Michigan University, Mount Pleasant, Michigan 48859, USA

<sup>5</sup>Department of Physics, Rikkyo University, 3-34-1 Nishi-Ikebukuro, Toshima, Tokyo 171-8501, Japan

<sup>6</sup>Department of Physics, University of Tokyo, Tokyo 1130033, Japan

(Received 19 June 2006; published 13 September 2006)

Excited states in  $^{40}\text{Si}$  have been established by detecting  $\gamma$  rays coincident with inelastic scattering and nucleon removal reactions on a liquid hydrogen target. The low excitation energy, 986(5) keV, of the  $2_1^+$  state provides evidence of a weakening in the  $N = 28$  shell closure in a neutron-rich nucleus devoid of deformation-driving proton collectivity.

DOI: [10.1103/PhysRevLett.97.112501](https://doi.org/10.1103/PhysRevLett.97.112501)

PACS numbers: 23.20.Lv, 21.10.Pc, 25.40.-h, 27.40.+z

The shell structure of the atomic nucleus provides one of the most important building blocks for the understanding of this correlated, fermionic many-body system [1,2]. Nuclei with a closed shell of protons or neutrons are particularly stable [3,4]. In neutron-rich exotic species, the shell structure, well-established close to stability, is modified; new magic numbers appear and some traditional shell gaps vanish [5,6]. Those changes in a regime of a pronounced imbalance between proton and neutron numbers are driven, for example, by the tensor force [7] and the proton-neutron monopole interaction [6,8,9].

A particularly fertile ground to study modifications to shell structure far from stability are neutron-rich nuclei with protons in the  $sd$  shell and neutrons in the  $fp$  shell [ $\pi(sd)\nu(fp)$ ]. The collapse of the  $N = 20$  shell closure in Ne, Na, and Mg isotopes is actively studied three decades after its discovery [10–18]. Prior experimental studies and theoretical predictions suggest a weakening of the  $N = 28$  magic number [19–22]. Coulomb excitation of the  $N = 28$  nucleus  $^{44}\text{S}$  implied enhanced collectivity [20] and  $\beta$ -decay experiments have been used to infer a deformed ground state [19]. The question of whether these observations are due to a breakdown of the  $N = 28$  magic number or the collapse of the  $Z = 16$  proton subshell gap at neutron number  $N = 28$  are much discussed in the literature [23,24]. A near-degeneracy of the  $\pi 1s_{1/2}$  and  $\pi 0d_{3/2}$  orbitals has been established experimentally for stable [25] and neutron-rich nuclei [26,27] at  $N = 28$ . However, observation of collectivity in these nuclei cannot be used to draw firm conclusions on the breakdown of  $N = 28$  because proton degeneracy also enhances collectivity approaching  $N = 28$ .

To isolate changes in the  $N = 28$  shell closure, we studied excited states in  $^{40}\text{Si}$  ( $Z = 14$ ,  $N = 26$ ) where recent experiments indicate the  $Z = 14$  proton subshell gap remains large at  $N = 28$  [26,27]. Thus, low-lying excited

states observed in  $^{40}\text{Si}$  probe predominantly neutron configurations, and the conclusions are not complicated by the proton degrees of freedom. Although a quasi-particle random-phase approximation analysis of  $\beta$ -decay half-lives suggests  $^{39-42}\text{Si}$  are deformed, confirmation by more direct methods is needed [28]. In the regime of exotic nuclei, excitation energies are often the first observables accessible to experiments. Two complementary reactions—proton inelastic scattering and nucleon removal—have been used in the present study to probe the level scheme of  $^{40}\text{Si}$ .

The experiment was carried out at the National Superconducting Cyclotron Laboratory (NSCL) at Michigan State University. A primary beam of  $^{48}\text{Ca}$  at 140 MeV/nucleon from the Coupled Cyclotron Facility (CCF) impinged upon a 987 mg/cm<sup>2</sup>  $^9\text{Be}$  target placed at the midacceptance position of the A1900 fragment separator [29]. Projectile fragments were then separated by the  $B\rho$ - $\Delta E$ - $B\rho$  method to deliver a cocktail beam composed of several nuclear species, including  $^{40}\text{Si}$ , to the target position of the S800 spectrograph [30]. The full acceptance of both the A1900 and the S800 analysis line, operated in focused mode, was used yielding a total momentum acceptance of 4%. At the S800 target position, the RIKEN/Kyushu/Rikkyo liquid hydrogen ( $\text{LH}_2$ ) target was placed into the path of the beam [31]. The spectrograph was set to accept projectile nuclei elastically scattered from protons in the target. Because of the large momentum acceptance of the spectrograph, single- and multiple-nucleon removal channels were also observed for many of the incoming nuclear species.

Prompt  $\gamma$ -ray decays of nuclei excited by inelastic scattering or left in an excited state by nucleon removal were detected by SeGA (Segmented Germanium Array), an array of 32-fold segmented, high-purity Ge detectors [32]. The array was configured around the  $\text{LH}_2$  target in

two rings with seven detectors at  $37^\circ$  and nine detectors at  $90^\circ$  relative to the beam axis. Event-by-event Doppler reconstruction takes advantage of the detector segmentation, producing  $\gamma$ -ray spectra in the projectile frame ( $v \sim 0.4c$ ) with  $\sim 3\%$  (FWHM) resolution at 1 MeV.

In thick-target, inverse-kinematics inelastic proton scattering, decay  $\gamma$  rays are used to tag inelastic scattering to specific excited states [33]. However, single- and multiple-nucleon removal reactions occur with comparable, or larger, cross sections. Thus, identification of both the incoming projectile and the outgoing nucleus is required. The charge of each incident projectile was determined for each event using a Si-PIN detector placed upstream at the object position of the S800, and an ionization chamber in the focal plane of the S800 determined the charge of each particle after the target [34]. The magnetic rigidity of each incident projectile was determined by measuring the dispersive angle at the intermediate image of the S800 analysis beam line using a pair of high-rate parallel plate avalanche counters. The magnetic rigidity of each particle exiting the target was determined by measuring the dispersive position of each particle in the S800 focal plane with a cathode readout drift chamber. Time of flight for each particle was measured between timing scintillators at the exit of the A1900 and the focal plane of the S800. Together, these kinematic measurements positively determined incoming mass and change in mass due to reactions.

Excited states of  $^{40}\text{Si}$  were populated by inelastic scattering of incoming  $^{40}\text{Si}$  nuclei and by  $pn$  removal from  $^{42}\text{P}$  upon collision with the  $\text{LH}_2$  target. Figure 1 shows projectile frame  $\gamma$ -ray spectra detected in coincidence with the reactions  $p(^{40}\text{Si}, ^{40}\text{Si} + \gamma)p'$  and  $p(^{42}\text{P}, ^{40}\text{Si} + \gamma)X$ . The transition at 986(5) keV is the strongest  $\gamma$  ray observed in

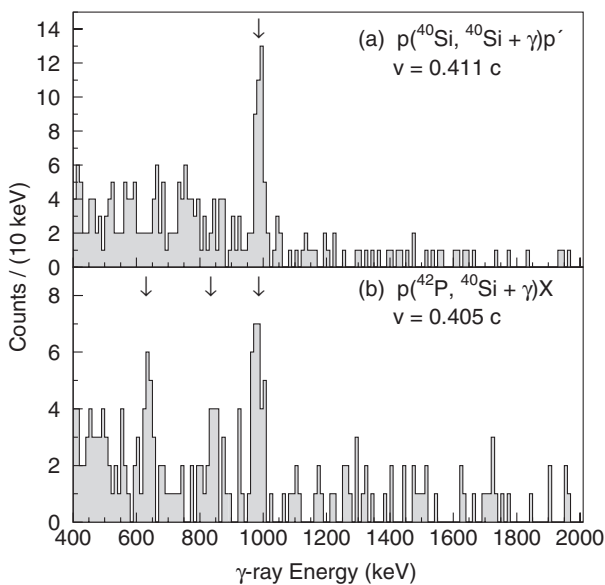


FIG. 1. Doppler-corrected  $\gamma$ -ray spectra observed in coincidence with the reactions  $p(^{40}\text{Si}, ^{40}\text{Si} + \gamma)p'$  and  $p(^{42}\text{P}, ^{40}\text{Si} + \gamma)X$ .

each of the reaction channels and the only transition observed via inelastic scattering. Its relative strength combined with the selectivity of  $(p, p')$  allow this transition to be assigned as the  $2_1^+ \rightarrow 0_1^+$  transition. Thus, the excitation energy of the first  $2_1^+$  state in  $^{40}\text{Si}$  is 986(5) keV.

The  $pn$  removal reaction leading to  $^{40}\text{Si}$  also shows two weaker peaks at 638(5) and 845(6) keV, each with about half the intensity of the corresponding  $2_1^+ \rightarrow 0_1^+$  transition. The energies of the 986(5) and 638(5) keV peaks agree with the observations of Grevy *et al.* [35]. The statistics obtained for the 638(5) and 845(6) keV transitions preclude a discussion of whether these two  $\gamma$ -ray transitions should be in parallel or form a cascade. However, they are expected to decay from higher excited states, based on other even-even nuclei that show significant  $\gamma$ -ray feeding of the  $2_1^+$  when populated by the  $pn$  removal reaction. Thus, we propose that at least one of these two lower-energy  $\gamma$  rays is directly feeding the  $2_1^+$  state and that an excited state of  $^{40}\text{Si}$  lies at either 1624(7) or 1831(8) keV.

Figure 2 shows the energy of the first  $2_1^+$  state,  $E(2_1^+)$ , versus neutron number ( $N = 22-26$ ) for even-even nuclei between silicon and chromium. Data in this figure were taken from the ENSDF database [36] and the current experiment. Figure 2(a) illustrates the evolution of  $E(2_1^+)$  in nuclei having large shell gaps for both  $N = 20$  and  $N = 28$ . Changes in the excitation energy are dominated by the filling of a single-neutron orbital,  $0f_{7/2}$ ; the trend is parabolic, reaching its minimum at midshell; and excitation energies are nearly symmetric about midshell,  $N = 24$ . In Fig. 2(b), this symmetry is lost. The lowering of first excited states in the neutron-rich sulfur and argon nuclei can be attributed, in part or in whole, to a narrowing of the

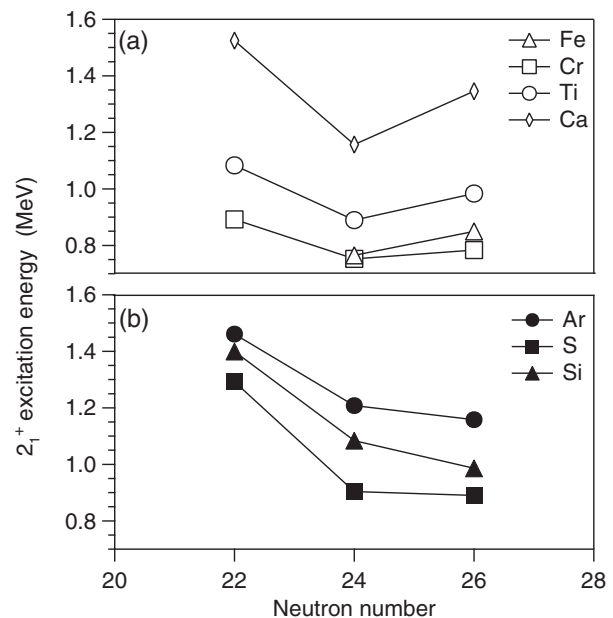


FIG. 2. Evolution of  $2_1^+$  energy with neutron number for even-even nuclei with  $Z \geq 20$  (a) and  $Z < 20$  (b).

$\pi(0d_{3/2} - 1s_{1/2})$  gap [23,24]. The rise in collectivity in the sulfur and argon nuclei is, therefore, not sufficient to establish a breakdown of the  $N = 28$  shell closure. The situation is quite different when considering the chain of silicon isotopes. Because  $Z = 14$  is a strong shell closure, the decrease in  $E(2_1^+)$  between  $^{38}\text{Si}$  and  $^{40}\text{Si}$  can only be due to a reduction of the  $N = 28$  shell gap.

To examine the decline in  $2_1^+$  energies across these neutron-rich silicon isotopes, large-scale shell-model calculations were performed with CMICHSM [37] in a  $\pi(sd)^{Z-8}\nu(fp)^{N-20}$  model space using the updated interaction of Nowacki and collaborators [23,38]. In Fig. 3, measured and predicted  $2_1^+$  excitation energies are plotted versus neutron number. While the evolution of excitation energies is in good agreement with experiment, the predicted values are consistently 450 keV higher than the measured values. The first excited state of each nucleus with  $15 \leq Z \leq 19$  and  $N = 22, 24, 26, 28$  has been measured and compared with shell-model predictions using the same interaction [23,38–40]. Agreement was quite good in all cases, and no other isotopic chain suffers from the large difference between prediction and theory observed in these silicon isotopes. Shell-model predictions reduced by an empirical offset of 450 keV are plotted in Fig. 3 as a dotted line. These shifted predictions give an rms error below 30 keV for  $^{36,38,40}\text{Si}$  and predict the  $2_1^+$  energy in  $^{42}\text{Si}$  at 1050 keV. This would place the  $2_1^+$  of  $^{42}\text{Si}$  below that of  $^{44}\text{S}$  in qualitative agreement with the observations of Greife *et al.* [35]. Because of the pronounced proton subshell closure at  $Z = 14$ , shell-model predictions indicate that the enhanced collectivity resulting from promotion of two neutrons across the  $N = 28$  shell gap will not result in strong deformation [41].

A possible explanation of the disagreement between theoretical predictions and experiment in the silicon  $2_1^+$

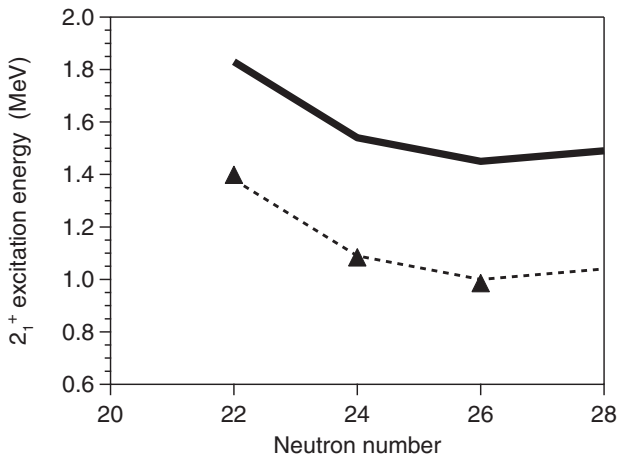


FIG. 3. Measured  $2_1^+$  energies ( $\Delta$ ) of  $^{36,38,40}\text{Si}$  with corresponding shell-model predictions (solid line) described in the text. Shell-model predictions shifted lower by 450 keV (dashed line) clearly reproduce the experimental values.

energies can be found in the neutron-rich carbon nuclei, which also have a strong proton subshell closure and initially showed a similar disagreement between theory and experiment. Measured and calculated spectra for  $^{18,20}\text{C}$  are shown in Fig. 4(a) [42,43]. By reducing the neutron-neutron ( $n$ - $n$ ) interaction strength in carbon, the WBPM interaction reproduces the observed level spacing better than WBP. In oxygen, the neutron orbital  $1s_{1/2}$  lies 0.87 MeV above the  $0d_{5/2}$  orbital at  $N = 9$ . This gap grows with increasing neutron number due to the  $n$ - $n$  interaction resulting in a shell gap at  $N = 14$  which makes  $^{22}\text{O}$  doubly magic [44]. In carbon, the neutron orbital  $1s_{1/2}$  lies 0.74 MeV below the  $0d_{5/2}$  orbital at  $N = 9$ . This orbital inversion leads WBP to predict  $N = 14$  is not a shell closure in carbon. The weaker  $n$ - $n$  interaction used in WBPM causes the  $\nu(1s_{1/2} - 0d_{5/2})$  gap to grow more slowly, thus reinforcing that no shell gap develops at  $N = 14$  in the carbon isotopes.

If we compare the oxygen and carbon chains to the calcium and silicon chains, the similarities are striking. Originally, shell-model calculations used the  $1p_{3/2} - 0f_{7/2}$  neutron gap of  $^{41}\text{Ca}$  with the  $n$ - $n$  interaction found in stable nuclei—which is known to widen the  $N = 28$

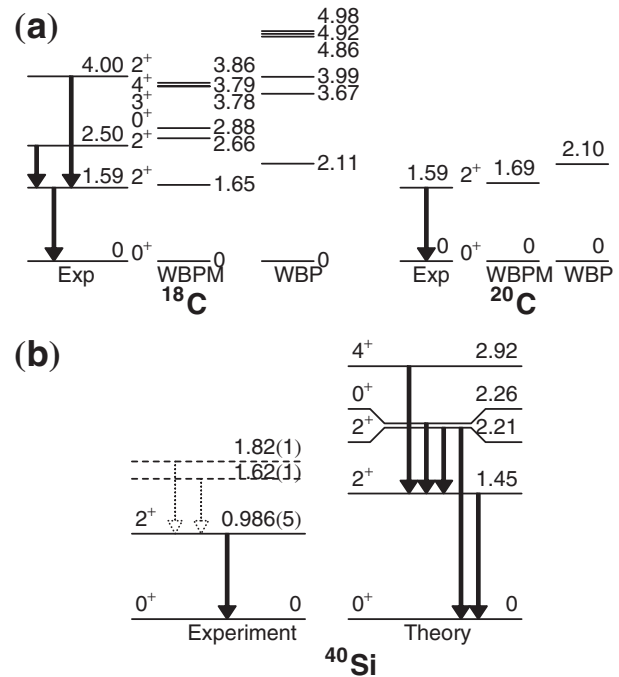


FIG. 4. Panel (a) shows the experimental level schemes of  $^{18,20}\text{C}$  along with shell-model predictions using the WBP and WBPM interactions. With the WBPM, reducing the valence  $n$ - $n$  interaction strength leads to better agreement with experiment. Panel (b) shows measured and predicted levels in  $^{40}\text{Si}$ . The two  $\gamma$  decay branches of the  $2_2^+$  state are predicted to have comparable intensities. The existence at a low excitation energy of one or both of the states predicted above the first  $2_1^+$  state would be consistent with the results of the present experiment. The experiment-theory shift is reminiscent of that seen in  $^{18,20}\text{C}$ .

shell gap—to predict  $^{42}\text{Si}$  as a doubly-magic nucleus [23]. Nummela *et al.* measured a reduction of this neutron gap in  $^{35}\text{Si}$  leading to a new prediction of weakened magicity in  $^{42}\text{Si}$  [38]. The current experiment shows that shell-model predictions give larger excitation spectrum spacing in silicon isotopes than is measured. Reducing the  $n$ - $n$  interaction at  $Z = 14$  could correct the predicted energy spacing but would also imply that the  $N = 28$  gap grows more slowly in silicon than in calcium and that current shell-model predictions are, in fact, overestimating the size of the  $N = 28$  shell gap. Experimental knowledge of higher lying states in the silicon isotopes is needed to fully examine this possible reduction in  $n$ - $n$  interaction strength.

Further support for a narrowing of the  $N = 28$  shell gap in  $^{40}\text{Si}$  comes from the low energy inferred here for the second excited state, independent of any specific interpretation of the experimental level scheme. In the shell model [compare Fig. 4(b)] the states predicted to decay through the  $2_1^+$  level, via  $\gamma$  rays of less than 1 MeV, arise from particle-hole excitations across the  $N = 28$  gap. Thus, their low excitation energy implies a reduced gap.

To summarize, the  $\gamma$  decays of excited states in  $^{40}\text{Si}$  have been observed using the complementary techniques of inelastic scattering and  $pn$  removal on a liquid hydrogen target. An excitation energy of 986(5) keV was measured for the  $2_1^+$  state in  $^{40}\text{Si}$ , and a second excited state at either 1624(7) or 1831(8) keV was deduced. The large proton subshell gap at  $Z = 14$  means that the evolution of excitation energies in the silicon isotopes is directly related to the narrowing of the  $N = 28$  shell gap. The decline in  $2_1^+$  energy from  $^{38}\text{Si}$ , at midshell, to  $^{40}\text{Si}$  can only be explained by a weakening of  $N = 28$ . The low energy of a second excited state in  $^{40}\text{Si}$  is compatible with shell-model predictions of particle-hole excitations across the  $N = 28$  shell gap. The  $2_1^+$  energy trend from shell-model calculations taken with an empirical shift predicts the first  $2^+$  energy in  $^{42}\text{Si}$  will be below that of  $^{44}\text{S}$ .

This work was supported by the National Science Foundation under Grants No. PHY-0110253, No. PHY-9875122, No. PHY-0244453, No. PHY-0555366, No. INT-0089581, and by the Japan Society for the Promotion of Science.

- 
- [1] E. Caurier *et al.*, *Rev. Mod. Phys.* **77**, 427 (2005).
  - [2] B. A. Brown, *Prog. Part. Nucl. Phys.* **47**, 517 (2001).
  - [3] M. G. Mayer, *Phys. Rev.* **75**, 1969 (1949).
  - [4] O. Haxel, J. H. D. Jensen, and H. E. Suess, *Phys. Rev.* **75**, 1766 (1949).
  - [5] D. Warner, *Nature (London)* **430**, 517 (2004).
  - [6] T. Otsuka *et al.*, *Phys. Rev. Lett.* **87**, 082502 (2001).

- [7] T. Otsuka *et al.*, *Phys. Rev. Lett.* **95**, 232502 (2005).
- [8] P. Federman, S. Pittel, and R. Campos, *Phys. Lett.* **82B**, 9 (1979).
- [9] K. Heyde *et al.*, *Phys. Lett. B* **155**, 303 (1985).
- [10] C. Thibault *et al.*, *Phys. Rev. C* **12**, 644 (1975).
- [11] X. Campi *et al.*, *Nucl. Phys.* **A251**, 193 (1975).
- [12] T. Motobayashi *et al.*, *Phys. Lett. B* **346**, 9 (1995).
- [13] B. V. Pritychenko *et al.*, *Phys. Lett. B* **461**, 322 (1999).
- [14] J. A. Church *et al.*, *Phys. Rev. C* **72**, 054320 (2005).
- [15] O. Niedermaier *et al.*, *Phys. Rev. Lett.* **94**, 172501 (2005).
- [16] V. Tripathi *et al.*, *Phys. Rev. Lett.* **94**, 162501 (2005).
- [17] G. Neyens *et al.*, *Phys. Rev. Lett.* **94**, 022501 (2005).
- [18] H. Iwasaki *et al.*, *Phys. Lett. B* **620**, 118 (2005).
- [19] O. Sorlin *et al.*, *Phys. Rev. C* **47**, 2941 (1993).
- [20] T. Glasmacher *et al.*, *Phys. Lett. B* **395**, 163 (1997).
- [21] T. Werner *et al.*, *Phys. Lett. B* **335**, 259 (1994); *Nucl. Phys.* **A597**, 327 (1996).
- [22] G. A. Lalazissis *et al.*, *Phys. Rev. C* **60**, 014310 (1999).
- [23] J. Retamosa, E. Caurier, F. Nowacki, and A. Poves, *Phys. Rev. C* **55**, 1266 (1997).
- [24] P. D. Cottle and K. W. Kemper, *Phys. Rev. C* **58**, 3761 (1998).
- [25] P. Doll *et al.*, *Nucl. Phys.* **A263**, 210 (1976).
- [26] J. Fridmann *et al.*, *Nature (London)* **435**, 922 (2005).
- [27] J. Fridmann *et al.*, *Phys. Rev. C* (to be published).
- [28] S. Grevy *et al.*, *Phys. Lett. B* **594**, 252 (2004).
- [29] D. J. Morrissey *et al.*, *Nucl. Instrum. Methods Phys. Res., Sect. B* **204**, 90 (2003).
- [30] D. Bazin *et al.*, *Nucl. Instrum. Methods Phys. Res., Sect. B* **204**, 629 (2003).
- [31] H. Ryuto *et al.*, *Nucl. Instrum. Methods Phys. Res., Sect. A* **555**, 1 (2005).
- [32] W. F. Mueller *et al.*, *Nucl. Instrum. Methods Phys. Res., Sect. A* **466**, 492 (2001).
- [33] H. Iwasaki *et al.*, *Phys. Lett. B* **481**, 7 (2000).
- [34] J. Yurkon *et al.*, *Nucl. Instrum. Methods Phys. Res., Sect. A* **422**, 291 (1999).
- [35] S. Grevy *et al.*, in *Direct Reactions with Exotic Beams 2005* (unpublished).
- [36] Data extracted using the NNDC On-Line Data Service from the ENSDF database, file revised as of March 30, 2006, [www.nndc.bnl.gov/ensdf](http://www.nndc.bnl.gov/ensdf).
- [37] M. Horoi, B. A. Brown, and V. Zelevinsky, *Phys. Rev. C* **67**, 034303 (2003).
- [38] S. Nummela *et al.*, *Phys. Rev. C* **63**, 044316 (2001).
- [39] D. Sohler *et al.*, *Phys. Rev. C* **66**, 054302 (2002).
- [40] A. Gade *et al.*, *Phys. Rev. C* (to be published).
- [41] E. Caurier, F. Nowacki, and A. Poves, *Nucl. Phys.* **A742**, 14 (2004).
- [42] M. Stanoiu *et al.*, *Nucl. Phys.* **A746**, 135c (2004).
- [43] E. K. Warburton and B. A. Brown, *Phys. Rev. C* **46**, 923 (1992).
- [44] B. A. Brown and W. A. Richter, *Phys. Rev. C* **72**, 057301 (2005).